Reactivity of Decamethylsamarocene with Polycyclic Aromatic Hydrocarbons[1]

William J. Evans,* Shirley L. Gonzales, and Joseph W. Ziller

Contribution from the Department of Chemistry, University of California, Irvine, Irvine, California 92717

*Received September 3, 1993**

Abstract: The reactivity of $(\eta^5\text{-}C_5Me_5)_2Sm$ (**1**) with polycyclic aromatic hydrocarbons and related nitrogen heterocycles has been examined. **1** reacts in arenes with substrates which have reduction potentials more positive than −2.22 V vs SCE to form a series of unusual bimetallic complexes in high yield. **1** reacts with anthracene to form $[(\eta^5\text{-}C_5Me_5)_2Sm]_2[\mu\text{-}\eta^3\text{:}\eta^3\text{-}(C_{14}H_{10})]$ (**2**) in which a planar $C_{14}H_{10}$ unit is coordinated on each side by a $(C_5Me_5)_2Sm$ moiety with shortest Sm–C distances of 2.595(4), 2.840(4), and 2.791(4) Å for the C(9), C(9a), and C(1) carbon atoms (anthracene numbering), respectively. Pyrene reacts with **1** to form $[(\eta^5\text{-}C_5Me_5)_2Sm]_2[\mu\text{-}\eta^3\text{:}\eta^3\text{-}(C_{16}H_{10})]$ (**3**) in which the two $(C_5Me_5)_2Sm$ units also coordinate to opposite sides of the planar polycyclic system, but they are on the same end of the tetracyclic unit. 2,3-Benzanthracene reacts with **1** to form an analog of **2**, $[(\eta^5\text{-}C_5Me_5)_2Sm]_2[\mu\text{-}\eta^3\text{:}\eta^3\text{-}(C_{18}H_{12})]$ (**4**). **1** also reacts with 9-methylanthracene and acenaphthylene to form $[(C_5Me_5)_2Sm]_2(C_{15}H_{12})$ (**5**) and $[(C_5Me_5)_2Sm]_2(C_{12}H_8)$ (**6**), respectively, in high yields. In contrast, the reaction of azulene with **1** generates $(\eta^5\text{-}C_5Me_5)_3Sm$. Phenazine reacts with **1** to produce $[(\eta^5\text{-}C_5Me_5)_2Sm]_2[\mu\text{-}\eta^3\text{:}\eta^3\text{-}(C_{12}H_8N_2)]$ (**7**), which is very similar to **2** except that it contains a 2.360(2) Å Sm–N bond. In contrast, acridine is reductively coupled by **1** to form $[(\eta^5\text{-}C_5Me_5)_2Sm]_2[\mu\text{-}\eta^3\text{:}\eta^3\text{-}(C_{13}H_9N)_2]$ (**8**), which contains nonplanar $C_{13}H_9N$ units. **2** crystallizes from toluene in the triclinic space group $P\bar{1}$ [C_i^1; No. 2] with unit cell parameters $a = 10.495(2)$ Å, $b = 11.2361(14)$ Å, $c = 11.2857(12)$ Å, $\alpha = 80.953(9)°$, $\beta = 85.463(11)°$, $\gamma = 76.657(12)°$, $V = 1277.6(3)$ Å^3, and $D_{calcd} = 1.445$ Mg m^{-3} for $Z = 1$. Least-squares refinement of the model based on 3298 reflections ($|F_o| > 0$) converged to a final $R_F = 2.8\%$. **3** crystallizes from benzene in the monoclinic space group $P2_1/n$ [C_{2h}^5; No. 14] with unit cell parameters $a = 16.528(2)$ Å, $b = 11.3716(16)$ Å, $c = 25.433(2)$ Å, $\beta = 101.194(9)°$, $V = 4689.1(10)$ Å^3, and $D_{calcd} = 1.479$ Mg m^{-3} for $Z = 4$. Least-squares refinement of the model based on 9373 observed reflections ($|F_o| > 3.0\sigma(|F_o|)$) converged to a final $R_F = 3.2\%$. **4** crystallizes from benzene in the triclinic space group $P\bar{1}$ [C_i^1; No. 2] with unit cell parameters $a = 10.2367(15)$ Å, $b = 11.174(3)$ Å, $c = 13.799(3)$ Å, $\alpha = 114.66(2)°$, $\beta = 92.200(13)°$, $\gamma = 110.45(2)°$, $V = 1312.2(5)$ Å^3, and $D_{calcd} = 1.453$ Mg m^{-3} for $Z = 1$. Least-squares refinement of the model based on 3051 reflections ($|F_o| > 6.0\sigma(|F_o|)$) converged to a final $R_F = 6.3\%$. **7** crystallizes from toluene in the triclinic space group $P\bar{1}$ [C_i^1; No. 2] with unit cell parameters $a = 10.5019(7)$ Å, $b = 11.1297(7)$ Å, $c = 11.4319(8)$ Å, $\alpha = 80.827(5)°$, $\beta = 76.846(5)°$, $\gamma = 86.149(5)°$, $V = 1283.483(15)$ Å^3, and $D_{calcd} = 1.441$ Mg m^{-3} for $Z = 1$. Least-squares refinement of the model based on 5776 reflections ($|F_o| > 0$) converged to a final $R_F = 2.7\%$. **8** crystallizes from benzene in the triclinic space group $P\bar{1}$ [C_i^1; No. 2] with unit cell parameters $a = 9.4639(9)$ Å, $b = 13.3525(12)$ Å, $c = 14.4497(13)$ Å, $\alpha = 71.790(7)°$, $\beta = 84.430(8)°$, $\gamma = 85.649(8)°$, $V = 1727.3(3)$ Å^3, and $D_{calcd} = 1.381$ Mg m^{-3} for $Z = 1$. Least-squares refinement of the model based on 4377 observed reflections ($|F_o| > 3.0\sigma(|F_o|)$) converged to a final $R_F = 2.7\%$.

Decamethylsamarocene, $(C_5Me_5)_2Sm$ (**1**) is one of the more reactive organolanthanide complexes known due to its strong reduction potential and unusual, sterically unsaturated, bent metallocene geometry.[2] As such, this complex is a good reagent with which both to probe the limits of f-element reactivity and to investigate the utility of lanthanides in developing new chemistry in other areas.[3] We report here on our efforts to pursue these two goals by studying the reactivity of $(C_5Me_5)_2Sm$ with polycyclic aromatic hydrocarbons and some related heterocyclic compounds containing nitrogen.

This study was initiated[1] in part to explore the capacity of lanthanides to interact with aromatic hydrocarbons. Traditionally, the lanthanide metals were not expected to form π-complexes with aromatic hydrocarbons due to the limited radial extension of their valence orbitals.[4] However, in recent years several crystallographically characterized lanthanide complexes have been reported which contain coordinated arene rings. These include $Sm(\eta^6\text{-}C_6Me_6)(AlCl_4)_3$,[5] $Sm[\eta^6\text{-}m\text{-}(Me)_2C_6H_4](AlCl_4)_3$,[6] and $Gd(\eta^6\text{-}Bu^t{}_3C_6H_3)_2$,[7] which exhibit η^6-arene coordination, and $[(C_5Me_5)_2Sm]_2(\mu\text{-}\eta^2\text{:}\eta^4\text{-}CH_2CHPh)$[8] and $[(C_5Me_5)_2Sm]_2(\mu\text{-}\eta^2\text{:}\eta^4\text{-}PhCHCHPh)$,[8] which display side-on coordination. We sought to determine if additional types of interactions with aromatic hydrocarbons were possible and how a more electronegative heteroatom would affect the coordination mode of the lanthanide.

Given the strong reduction potential of $(C_5Me_5)_2Sm$, these reactions could produce polycyclic aromatic hydrocarbon anions, an area for which there is a dearth of structural information. Given the structural flexibility exhibited by the $(C_5Me_5)_2Sm$ unit in a variety of systems[9–11] we sought to explore the utility of this metallocene in isolating crystallographically characterizable

* Abstract published in *Advance ACS Abstracts*, January 15, 1994.

(1) Reported in part at the 203rd ACS National Meeting, San Francisco, CA, April 1992, INOR 633.

(2) (a) Evans, W. J.; Hughes, L. A.; Hanusa, T. P. *J. Am. Chem. Soc.* **1984**, *106*, 4270–4272. (b) Evans, W. J.; Hughes, L. A.; Hanusa, T. P. *Organometallics* **1986**, *5*, 1285–1291.

(3) Evans, W. J. *Polyhedron* **1987**, *6*, 803–835.

(4) (a) Freeman, A. J.; Watson, R. E. *Phys. Rev.* **1976**, *9*, 217. (b) Moeller, T. *Comprehensive Inorganic Chemistry*; Bailar, J. C., Jr. Ed.; Pergamon Press: Oxford, England, 1973; Vol. 4, Chapter 44.

(5) (a) Cotton, A.; Schwotzer, W. *J. Am. Chem. Soc.* **1986**, *108*, 4657–4658. (b) Cotton, A.; Schwotzer, W. *Organometallics* **1987**, *6*, 1275–1280.

(6) (a) Fan, B.; Shen, Q.; Lin, Y. *J. Organomet. Chem.* **1989**, *376*, 61–66. (b) Fan, B.; Shen, Q.; Lin, Y. *J. Organomet. Chem.* **1989**, *377*, 51–58.

(7) Brennan, J. G.; Cloke, F. G. N.; Sameh, A. A.; Zalkin, A. *J. Chem. Soc., Chem. Commun.* **1987**, 1668–1669.

(8) Evans, W. J.; Ulibarri, T. A.; Ziller, J. W. *J. Am. Chem. Soc.* **1990**, *112*, 219–223.

(9) Evans, W. J.; Drummond, D. K.; Hughes, L. A.; Zhang, H.; Atwood, J. L. *Polyhedron* **1988**, *7*, 1693–1703.

(10) Evans, W. J.; Kociok-Köhn, G.; Foster, S. E.; Ziller, J. W.; Doedens, R. J. *J. Organomet. Chem.* **1993**, *444*, 61–66.

0002-7863/94/1516-2600$04.50/0

Table 1. Crystallographic Data for $[(\eta^5\text{-}C_5Me_5)_2Sm]_2[\mu\text{-}\eta^3\text{:}\eta^3\text{-}(C_{14}H_{10})]$ (**2**), $[(\eta^5\text{-}C_5Me_5)_2Sm]_2[\mu\text{-}\eta^3\text{:}\eta^3\text{-}(C_{16}H_{10})]$ (**3**), and $[(\eta^5\text{-}C_5Me_5)_2Sm]_2[\mu\text{-}\eta^3\text{:}\eta^3\text{-}(C_{18}H_{12})]$[(**4**)[a]

complex	**2**	**3**	**4**
formula	$C_{54}H_{70}Sm_2\cdot C_7H_8$	$C_{56}H_{70}Sm_2$	$C_{58}H_{72}Sm_2\cdot C_6H_6$
mol wt	1111.9	1043.8	1148.0
crystal system	triclinic	monoclinic	triclinic
space group	$P\bar{1}$ [C_i^1; No. 2]	$P2_1/n$ [C_{2h}^5; No. 14]	$P\bar{1}$ [C_i^1; No. 2]
cell constants			
a, Å	10.495 (2)	16.528(2)	10.2367(15)
b, Å	11.2361(14)	11.3716(16)	11.174(3)
c, Å	11.2857(12)	25.433(2)	13.799(3)
α, deg	80.953(9)		114.66(2)
β, deg	85.463(11)	101.194(9)	92.200(13)
γ, deg	76.657(12)		110.45(2)
cell vol, Å^3	1277.6(3)	4689.1(10)	1312.2(5)
moles/unit cell	1	4	1
D_{calcd}, Mg m^{-3}	1.445	1.479	1.453
temp, K	178	158	168
μ_{calcd}, mm^{-1}	2.32	2.523	2.261
transmission, coeff (min–max)	0.5728–1.0000	0.2986–0.3733	0.8396–0.9841
R_F, %	2.8	3.2	6.3
R_{wF}, %	3.5	4.6	7.9
GOF	1.72	1.12	3.27

[a] Radiation for all structures was Mo Kα; λ = 0.710 730 Å.

complexes containing reduced aromatics. Furthermore, by examining a series of polycyclic aromatic hydrocarbons, we could gain information about the effective reducing power[12] of $(C_5Me_5)_2Sm$ in the generation of isolable systems and its capacity to reduce or reductively couple unsaturated substrates. We report here the several ways in which $(C_5Me_5)_2Sm$ can react with polycyclic aromatic hydrocarbons and the unusual structures which result.

Experimental Section

The complexes described below are extremely air- and moisture-sensitive. Therefore, both the syntheses and subsequent manipulations of these compounds were conducted under nitrogen or argon with rigorous exclusion of air and water by using Schlenk, vacuum line, and glovebox (Vacuum/Atmospheres HE-553 or HE-43-2 Dri-Lab) techniques. Solvents were purified and physical measurements were obtained as previously described.[13] Anthracene, 2,3-benzanthracene, azulene, phenazine, acridine, and coronene (Aldrich) were used without further purification. Pyrene, 9-methylanthracene, and acenaphthylene (Aldrich) were sublimed (100 °C, 10^{-5} Torr) prior to use. $(C_5Me_5)_2Sm$ was synthesized according to the literature and handled in an ether-free glovebox under argon.[2] NMR spectra were obtained on General Electric QE-300 and GN-500 MHz spectrometers. Elemental analyses were performed at Analytische Laboratorien GmbH, Gummersbach, Germany.

$[(\eta^5\text{-}C_5Me_5)_2Sm]_2[\mu\text{-}\eta^3\text{:}\eta^3\text{-}(C_{14}H_{10})]$ (2). In the glovebox, anthracene (9 mg, 0.05 mmol) was added to green $(C_5Me_5)_2Sm$ (42 mg, 0.10 mmol) in toluene (2 mL). The solution immediately turned darker green. After the mixture was stirred for 5 min, the solvent was removed by rotary evaporation to yield **2** as a black microcrystalline solid (51 mg, 90%). ^{1}H NMR (C_6D_6) δ 1.42 (C_5Me_5), 1.26 (C_5Me_5) (resonances assignable to $C_{14}H_{10}$ could not be identified due to the paramagnetism of the metal). ^{13}C NMR (C_6D_6) δ 125.6 (C_5Me_5), 21.4 (C_5Me_5). IR (KBr) 2910 s, 2854 s, 1570 w, 1560 w, 1449 s, 1378 w, 1287 m, 882 m, 728 s cm^{-1}. Anal. Calcd for $Sm_2C_{54}H_{70}$: C, 63.59; H, 6.92; Sm, 29.49. Found: C, 63.45; H, 6.78; Sm, 29.25. Crystals suitable for an X-ray diffraction study were obtained by slow concentration of a toluene solution.

X-ray Data Collection, Structure Determination, and Refinement for $[(\eta^5\text{-}C_5Me_5)_2Sm]_2[\mu\text{-}\eta^3\text{:}\eta^3\text{-}(C_{14}H_{10})]$ (2). A red crystal of approximate dimensions 0.20 × 0.25 × 0.31 mm was immersed in Paratone D, mounted on a glass fiber, and transferred to the Siemens P3 diffractometer which is equipped with a modified LT-2 low temperature system. Determination of Laue symmetry, crystal class, unit cell parameters, and the crystal's orientation matrix were carried out by previously described techniques similar to those of Churchill.[14] Low-temperature (178 K) intensity data were collected via a θ–2θ scan technique with Mo Kα radiation under the conditions given in Table 1. All 3581 data were corrected for absorption and for Lorentz and polarization effects and placed on an approximately absolute scale. Any reflection with I(net) < 0 was assigned the value $|F_o| = 0$. There were no systematic extinctions nor any diffraction symmetry other than the Friedel condition. The two possible triclinic space groups are the noncentrosymmetric $P1$ [C_1^1; No. 1] or the centrosymmetric $P\bar{1}$ [C_i^1; No. 2]. With no expectation of a resolved chiral molecule, the latter centrosymmetric space group is far more probable,[15] and was later shown to be the correct choice.

All crystallographic calculations were carried out using either the UCI modified version of the UCLA Crystallographic Computing Package[16] or the SHELXTL PLUS program set.[17] The analytical scattering factors for neutral atoms were used throughout the analysis;[18a] both the real ($\Delta f'$) and the imaginary ($i\Delta f''$) components of anomalous dispersion[18b] were included. The quantity minimized during least-squares analysis was $\Sigma w(|F_o| - |F_c|)^2$ where $w^{-1} = \sigma^2(|F_o|) + 0.0003(|F_o|)^2$. The absorption correction was done using a semiempirical ψ scan method and XEMP.[17]

The structure was solved by direct methods (SHELXTL PLUS)[17] and refined by full-matrix least-squares techniques. The molecule is a dimer and is located about a crystallographic inversion center at (0,1,0). Hydrogen atoms were included using a riding model with d(C–H) = 0.96 Å and U(iso) = 0.08 Å^2. There is a disordered toluene molecule present which is located about an inversion center ($^1/_2$,0,$^1/_2$). The eight hydrogen atoms of the toluene molecule were not included in the refinement. Refinement of the model led to convergence with R_F = 2.8%, R_{wF} = 3.5%, and GOF = 1.72 for 274 variables refined against all 3298 data with $|F_o| > 0$. A final difference–Fourier map yielded ρ(max) = 1.02 eÅ^{-3}.

$[(\eta^5\text{-}C_5Me_5)_2Sm]_2[\mu\text{-}\eta^3\text{:}\eta^3\text{-}(C_{16}H_{10})]$ (3). In the glovebox, pyrene (14 mg, 0.07 mmol) was added to $(C_5Me_5)_2Sm$ (57 mg, 0.14 mmol) in toluene (2 mL). The solution immediately turned bright green. After the mixture was stirred for 5 min, the solvent was removed by rotary evaporation to yield **3** as a dark green, almost black, microcrystalline solid (71 mg, 99%). ^{1}H NMR (C_6D_6) δ 1.08 (C_5Me_5). ^{13}C NMR (C_6D_6) δ 105.2 (C_5Me_5), 20.2 (C_5Me_5). IR (KBr) 2906 s, 2858 s, 2362 m, 1654 w, 1559 m, 1541 m, 1507 m, 1436 s, 1380 m, 1183 w, 1021 w, 842 s, 747 m, 711 s, 676 m cm^{-1}. Anal. Calcd for $Sm_2C_{56}H_{70}$: C, 64.43; H, 6.76; Sm, 28.81. Found: C, 64.11; H, 6.58.; Sm, 29.20. Crystals suitable for an X-ray diffraction study were obtained by slow concentration of a benzene solution.

(11) Evans, W. J.; Kociok-Köhn, G.; Ziller, J. W. *Angew. Chem., Int. Ed. Engl.* **1992**, *31*, 1081–1082.

(12) An estimate of –2.4 V has been cited: Finke, R. G.; Keenan, S. R.; Schiraldi, D. A.; Watson, P. L. *Organometallics* **1986**, *5*, 598–601.

(13) (a) Evans, W. J.; Chamberlain, L. R.; Ulibarri, T. A.; Ziller, J. W. *J. Am. Chem. Soc.* **1988**, *110*, 6423–6432. (b) Evans, W. J.; Ulibarri, T. A.; Chamberlain, L. R.; Ziller, J. W.; Alvarez, D., Jr. *Organometallics* **1990**, *9*, 2124–2130.

(14) Churchill, M. R.; Lashewycz, R. A.; Rotella, F. J. *Inorg. Chem.* **1977**, *16*, 265–271.

(15) Nowacki, W.; Matsumoto, T.; Edenharter, A. *Acta Crystallogr.* **1967**, *22*, 935–940.

(16) *UCLA Crystallographic Computing Package*; University of California Los Angeles, 1981, Strouse, C., personal communication.

(17) Sheldrick, G. M. Siemens Analytical X-Ray Instruments, Inc.; Madison, WI 1990.

(18) *International Tables for X-Ray Crystallography*; Kynoch Press: Birmingham, England, 1974; (a) pp 99–101, (b) pp 149–150.

X-ray Data Collection, Structure Determination, and Refinement for $[(\eta^5\text{-}C_5Me_5)_2Sm]_2[\mu\text{-}\eta^3\text{:}\eta^3\text{-}(C_{16}H_{10})]$ (**3**). A dark purple crystal of approximate dimensions 0.36 × 0.40 × 0.50 mm was handled as described above for **2**. Intensity data were collected at 158 K and all 11757 data were corrected as described above for **2** (Table 1). The diffraction symmetry was $2/m$ with systematic absences $0k0$ for $k = 2n + 1$ and $h0l$ for $h + l = 2n + 1$. The centrosymmetric monoclinic space group $P2_1/n$ [C_{2h}^5; No. 14] is therefore uniquely defined.

The structure was solved by direct methods and refined by full-matrix least-squares techniques. Hydrogen atoms were included as for **2**. The quantity minimized during least-squares analysis was $\Sigma w(|F_o| - |F_c|)^2$ where $w^{-1} = \sigma^2(|F_o|) + 0.0010(|F_o|)^2$. Refinement of positional and thermal parameters led to convergence with $R_F = 3.2\%$, $R_{wF} = 4.6\%$, and GOF = 1.12 for 523 variables refined against those 9373 data with $|F_o| > 3.0\sigma(|F_o|)$. A final difference-Fourier synthesis showed no significant features, with $\rho(\max) = 0.73$ eÅ^{-3}.

$[(\eta^5\text{-}C_5Me_5)_2Sm]_2[\mu\text{-}\eta^3\text{:}\eta^3\text{-}(C_{18}H_{12})]$ (**4**). In the glovebox, 2,3-benzanthracene (13 mg, 0.055 mmol) was added to $(C_5Me_5)_2Sm$ (47 mg, 0.11 mmol) in toluene (2 mL). The solution immediately turned darker green, and after 5 min of stirring the solvent was removed by rotary evaporation to yield **4** as a Kelly green microcrystalline solid (58 mg, 98%). ^{1}H NMR (C_6D_6) δ 1.43 (C_5Me_5), 1.11 (C_5Me_5). ^{13}C NMR (C_6D_6) δ 117.0 (C_5Me_5), 17.5 (C_5Me_5). IR (KBr) 2918 s, 2856 s, 1449 s, 1435 s, 1315 w, 1175 w, 790 m, 739 m cm^{-1}. Anal. Calcd for $Sm_2C_{58}H_{72}$: C, 65.11; H, 6.78; Sm, 28.11. Found: C, 64.77; H, 6.60; Sm, 27.20. X-ray quality crystals were obtained by slow evaporation of a benzene solution.

X-ray Data Collection, Structure Determination, and Refinement for $[(\eta^5\text{-}C_5Me_5)_2Sm]_2[\mu\text{-}\eta^3\text{:}\eta^3\text{-}(C_{18}H_{12})]$ (**4**). A purple crystal of approximate dimensions 0.18 × 0.18 × 0.20 mm was handled as described above for **2**. Low-temperature (168 K) intensity data were collected and all 3665 data were corrected as described above for **2** (Table 1). The two possible triclinic space groups are the noncentrosymmetric $P1$ [C_1^1; No. 1] or the centrosymmetric $P\bar{1}$ [C_i^1; No. 2]. Refinement of the model using the centrosymmetric space group proved it to be the correct choice.

The structure was solved by direct methods (SHELXTL PLUS)[17] and refined by full-matrix least-squares techniques. The quantity minimized during least-squares analysis was $\Sigma w(|F_o| - |F_c|)^2$ where $w^{-1} = \sigma^2(|F_o|) + 0.0003(|F_o|)^2$. The molecule is a dimer which is located on an inversion center (0,0,0). There is one molecule of benzene present per dimeric unit (the benzene denoted by carbon atoms C(30) to C(32) is centered about an inversion center (0,0,$^1/_2$)). Hydrogen atoms were included as for **2**. Refinement of the model led to convergence with $R_F = 6.3\%$, $R_{wF} = 7.9\%$, and GOF = 3.27 for 247 variables refined against those 3051 data with $|F_o| > 6.0\sigma(|F_o|)$. A final difference-Fourier map yielded $\rho(\max) = 5.74$ eÅ^{-3}.

The structure has a few problems which must be noted. The cyclopentadienyl ring C(1)–C(10) was refined with isotropic temperature factors because C(4) and C(9) became non-positive-definite during refinement. Even when refined in this manner, the C(4) thermal parameter did not refine well, the resulting in a low value (0.003 Å^2). The C(4) thermal parameter was then fixed at 0.03 Å^2. This value was chosen since it is consistent with the other (C(1)–C(5)) ring carbon thermal parameters which range from 0.020 to 0.033 Å^2. There is some unaccounted for residual electron density near carbon atoms C(12) and C(13). The largest difference-peak is 5.74 eÅ^{-3} at a distance of 1.64 Å from C(12) and 1.62 Å from C(13). This residual density makes no crystallographic or chemical sense and may be attributed to a small satellite crystal. There were a few spurious intensities on the axial photographs but it was decided to proceed with this crystal since it was the best one available. It is believed that the above problems do not severely compromise the results of this structural determination which is otherwise complete and correct.

$[(C_5Me_5)_2Sm]_2(C_{15}H_{12})$ (**5**). In the glovebox, 9-methylanthracene (7 mg, 0.035 mmol) was added to $(C_5Me_5)_2Sm$ (30 mg, 0.07 mmol) in toluene (2 mL). The solution immediately turned wine red, and after 5 min of stirring the solvent was removed by rotary evaporation to yield **5** as a wine red glassy solid (36 mg, 99%). ^{1}H NMR (C_6D_6) δ 1.17 (C_5Me_5). ^{13}C NMR (C_6D_6) δ 120.5 (C_5Me_5), 20.3 (C_5Me_5). IR (KBr) 2904 s, 2856 m, 1556 w, 1538 w, 1419 s, 1331 m, 793 m, 698 m, 676 s, 653 m cm^{-1}. Anal. Calcd for $Sm_2C_{55}H_{72}$: C, 63.89; H, 7.02; Sm, 29.09. Found: C, 63.63; H, 6.86; Sm, 29.35.

$[(C_5Me_5)_2Sm]_2(C_{12}H_8)$, (**6**). In the glovebox, acenaphthylene (8 mg, 0.05 mmol) was added to $(C_5Me_5)_2Sm$ (43 mg, 0.10 mmol) in benzene (2 mL). The solution immediately turned indigo blue, and after 5 min of stirring the solvent was removed by rotary evaporation to give a quantitative yield of **6** as a dark blue, microcrystalline solid. ^{1}H NMR (C_6D_6) δ 1.03 (C_5Me_5), 0.52 (C_5Me_5). ^{13}C NMR (C_6D_6) δ 117.7 (C_5Me_5), 17.4 (C_5Me_5). IR (KBr) 2965 m, 2918 s, 2855 m, 1438 m, 1408 m, 1316 w, 1261 m, 1090 s, 1019 m, 802 s, 777 w, 707 w, 684 m cm^{-1}. Anal. Calcd for $Sm_2C_{52}H_{68}$: C, 62.84; H, 6.90; Sm, 30.26. Found: C, 61.78; H, 6.74; Sm, 29.60.

Table 2. Crystallographic Data for $[(\eta^5\text{-}C_5Me_5)_2Sm]_2[\mu\text{-}\eta^3\text{:}\eta^3\text{-}(C_{12}H_8N_2)]$ (**7**) and $[(\eta^5\text{-}C_5Me_5)_2Sm]_2[\mu\text{-}\eta^3\text{:}\eta^3\text{-}(C_{13}H_9N)_2]$ (**8**)[a]

complex	7	8
formula	$C_{52}H_{68}N_2Sm_2\cdot C_7H_8$	$C_{66}H_{78}N_2Sm_2$
mol wt	1113.9	1434.3
crystal system	triclinic	triclinic
space group	$P\bar{1}$ [C_i^1; No. 2]	$P\bar{1}$ [C_i^1; No. 2]
cell constants		
a, Å	10.5019(7)	9.4639(9)
b, Å	11.1297(7)	13.3525(12)
c, Å	11.4319(8)	14.4497(13)
α, deg	80.827(5)	71.790(7)
β, deg	76.846(5)	84.430(8)
γ, deg	86.149(5)	85.649(8)
cell vol, Å^3	1283.83(15)	1727.3(3)
moles/unit cell	1	1
D_{calcd}, Mg m^{-3}	1.441	1.381
temp, K	173	173
μ_{calcd}, mm^{-1}	2.31	1.736
transmission, coeff (min–max)	0.4825–0.5836	0.6108–0.7217
R_F, %	2.7	2.7
R_{wF}, %	3.4	4.6
GOF	1.09	4.56

[a] Radiation for all structures was Mo Kα; λ = 0.710 730 Å.

$[(\eta^5\text{-}C_5Me_5)_2Sm]_2[\mu\text{-}\eta^3\text{:}\eta^3\text{-}(C_{12}H_8N_2)]$ (**7**). In the glovebox, phenazine (7 mg, 0.04 mmol) was added to $(C_5Me_5)_2Sm$ (32 mg, 0.08 mmol) in toluene (2 mL). The solution immediately turned reddish-brown. After the mixture was stirred for 5 min, the solvent was removed by rotary evaporation to give a quantitative yield of **7** as a dark brown microcrystalline solid. ^{1}H NMR (C_6D_6) δ 1.38 (C_5Me_5). ^{13}C NMR (C_6D_6) δ 120.7 (C_5Me_5), 20.9 (C_5Me_5). IR (KBr) 2910 s, 2857 s, 1517 m, 1507 m, 1458 s, 1304 w, 1283 w cm^{-1}. Anal. Calcd for $Sm_2C_{52}H_{68}N_2$: C, 61.12; H, 6.71; N, 2.74; Sm, 29.43. Found: C, 60.55; H, 6.60; N, 2.58; Sm, 30.15. Crystals suitable for an X-ray diffraction study were obtained by slow concentration of a toluene solution.

X-ray Data Collection, Structure Determination, and Refinement for $[(\eta^5\text{-}C_5Me_5)_2Sm]_2[\mu\text{-}\eta^3\text{:}\eta^3\text{-}(C_{12}H_8N_2)]$ (**7**). A red crystal of approximate dimensions 0.13 × 0.23 × 0.27 mm was handled as described for **2** and transferred to the Syntex $P2_1$ (Siemens P3 system) diffractometer which is equipped with a modified LT-1 low-temperature system. Low-temperature (173 K) intensity data were collected and all 6256 data were corrected as described for **2** (Table 2). Any reflection with $I(\text{net}) < 0$ was assigned the value $|F_o| = 0$. There were no systematic extinctions nor any diffraction symmetry other than the Friedel condition. The two possible triclinic space groups are the noncentrosymmetric $P1$ [C_1^1; No. 1] or the centrosymmetric $P\bar{1}$ [C_i^1; No. 2]. With no expectation of a resolved chiral molecule, the latter centrosymmetric space group is far more probable,[15] and was later shown to be the correct choice.

The structure was solved by direct methods (SHELXTL PLUS)[17] and refined by full-matrix least-squares techniques. The quantity minimized during least-squares analysis was $\Sigma w(|F_o| - |F_c|)^2$ where $w^{-1} = \sigma^2(|F_o|) + 0.0006(|F_o|)^2$. The molecule is a dimer and is located about a crystallographic inversion center at ($^1/_2$,$^1/_2$,$^1/_2$). Hydrogen atoms were included as described for **2**. There is a disordered toluene molecule present which is located about an inversion center (0,0,$^1/_2$). The eight hydrogen atoms of the toluene molecule were not included in the refinement. Refinement of the model led to convergence with $R_F = 2.7\%$, $R_{wF} = 3.4\%$, and GOF = 1.09 for 299 variables refined against all 5776 data with $|F_o| > 0$. A final difference-Fourier map yielded $\rho(\max) = 0.51$ eÅ^{-3}.

$[(\eta^5\text{-}C_5Me_5)_2Sm]_2[\mu\text{-}\eta^3\text{:}\eta^3\text{-}(C_{13}H_9N)_2]$ (**8**). In the glovebox, acridine (11 mg, 0.06 mmol) was added to $(C_5Me_5)_2Sm$ (25 mg, 0.06 mmol) in toluene (2 mL). The solution immediately turned orange. After the mixture was stirred for 5 min, the solvent was removed by rotary evaporation to leave a dark red oil. The oil was extracted with a small amount of benzene and centrifuged. The solution was decanted and the solvent was removed by rotary evaporation to yield **8** as an orange solid (37 mg, 96%). ^{1}H NMR (C_6D_6) δ 0.67 (C_5Me_5), 0.40 (C_5Me_5). ^{13}C NMR (C_6D_6) δ 120.9 (C_5Me_5), 21.3 (C_5Me_5). IR (KBr) 3738 m, 3375

Table 3. Reactivity of Hydrocarbons with $(\eta^5\text{-}C_5Me_5)_2Sm$, **1**

hydrocarbon	$-E_{1/2}$[a]	$-E_{1/2}'$[a]	reaction with **1** obsd	color of product	ref
naphthalene	2.60		no		*b*
stilbene	2.22		yes	maroon-red	8
pyrene	2.10		yes	blue green	*b*
coronene	2.05	2.44	no[c]		*b*
anthracene	1.98	2.44	yes	green (purple solid)	*b*
cyclooctatetraene	1.83	1.99	yes	orange	21
acenaphthylene	1.65	1.89	yes	indigo blue	*b*
azulene	1.63	2.33	yes	red-brown	*b*
2,3-benzanthracene	1.58	1.93	yes	kelly green	*b*

[a] In volts relative to the saturated calomel electrode. $-E_{1/2}$ and $-E_{1/2}'$ describe the first and second reduction potentials of the hydrocarbon, respectively.[20] [b] This work. [c] The low solubility of coronene may inhibit the reaction.

m, 2913 s, 2863 s, 2363 m, 2343 w, 1606 w, 1581 w, 1544 w, 1506 w, 1475 s, 1463 m, 1325 s, 1300 s, 756 s, 738 s cm^{-1}. Anal. Calcd for $Sm_2C_{66}H_{78}N_2$: C, 66.05; H, 6.55; N, 2.34; Sm, 25.06. Found: C, 65.81; H, 6.37; N, 2.39; Sm, 24.60. Crystals suitable for an X-ray diffraction study were obtained by slow concentration of a benzene solution.

X-ray Data Collection, Structure Determination, and Refinement for $[(\eta^5\text{-}C_5Me_5)_2Sm]_2[\mu\text{-}\eta^3\text{:}\eta^3\text{-}(C_{13}H_9N)_2]$ (8). An orange crystal of approximate dimensions 0.33 × 0.37 × 0.43 mm was handled as described for **2**. Low-temperature (173 K) intensity data were collected and all 4865 data were corrected as described for **2** (Table 2). Any reflection with $I(\text{net}) < 0$ was assigned the value $|F_o| = 0$. There were no systematic extinctions nor any diffraction symmetry other than the Friedel condition. The two possible triclinic space groups are the noncentrosymmetric $P1$ [C_1^1; No. 1] or the centrosymmetric $P\bar{1}$ [C_i^1; No. 2]. Refinement of the model using the centrosymmetric space group proved it to be the correct choice.

The crystallographic calculations were carried out as described for **2**. The structure was solved by direct methods (SHELXTL PLUS)[17] and refined by full-matrix least-squares techniques. The quantity minimized during least-squares analysis was $\Sigma w(|F_o| - |F_c|)^2$ where $w^{-1} = \sigma^2(|F_o|) + 0.00005(|F_o|)^2$. The molecule is a dimer which is located on an inversion center ($^1/_2$,0,0). There are three molecules of benzene present per dimeric unit (the benzene denoted by carbon atoms C(41) to C(43) is centered about an inversion center ($^1/_2$,$^1/_2$,$^1/_2$). The hydrogen atoms were included as described for **2**. Refinement of the model led to convergence with $R_F = 2.7\%$; $R_{wF} = 4.6\%$, and GOF = 4.56 for 398 variables refined against those 4377 data with $|F_o| > 3.0\sigma(|F_o|)$. A final difference-Fourier map yielded $\rho(\text{max}) = 1.08$ eÅ^{-3}.

Results

The reactivity of $(C_5Me_5)_2Sm$ (**1**) with a series of aromatic hydrocarbons of increasing size was systematically examined starting with benzene. No evidence for formation of an isolable complex of $(C_5Me_5)_2Sm$ with benzene or toluene has been observed, although the variation of the ^{1}H NMR spectral line widths in these two solvents suggests that some interaction may occur.[2] Crystallizations of $(C_5Me_5)_2Sm$ from these solvents yield either crystals of the unsolvated bent metallocene[2] or the dinitrogen complex, $[(C_5Me_5)_2Sm]_2(\mu\text{-}\eta^2\text{:}\eta^2\text{-}N_2)$.[19] No reaction between $(C_5Me_5)_2Sm$ and naphthalene is observed at ambient temperature or in toluene at reflux. $(C_5Me_5)_2Sm$ does react with polycyclic aromatic hydrocarbons the size of anthracene and larger, however. The reactivity is summarized in Table 3 and is described in detail in the following sections.

The Anthracene Reaction. Formation of $[(\eta^5\text{-}C_5Me_5)_2Sm]_2[\mu\text{-}\eta^3\text{:}\eta^3\text{-}(C_{14}H_{10})]$ (2). When 0.5 equiv of anthracene is added to a dark green solution of **1** in toluene, the solution immediately darkens. Within 5 min, a black microcrystalline product can be isolated in quantitative yield by removal of solvent. Elemental analysis was consistent with the formation of **2** according to eq 1. The ^{1}H NMR spectrum of **2** in benzene showed two resonances

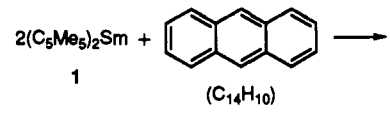

$$[(C_5Me_5)_2Sm]_2[\mu\text{-}\eta^3\text{:}\eta^3\text{-}(C_{14}H_{10})] \quad (1)$$
2

of equal intensity in the C_5Me_5 region and the ^{13}C NMR spectrum was indicative of C_5Me_5 moieties in a Sm(III) complex.[22] Resonances assignable to the $C_{14}H_{10}$ moiety were not identifiable due to the paramagnetism of the metal as is often the case for non-cyclopentadienyl ligands in organosamarium complexes. **2** dissolves in THF to regenerate anthracene and form $(C_5Me_5)_2Sm(THF)_2$. Since these data were not structurally definitive, an X-ray diffraction study was conducted.

Although **2** is only sparingly soluble in arenes, it was soluble enough to provide X-ray quality crystals by slow evaporation of a toluene solution. The crystal structure was consistent with the analytical data and revealed the unusual bimetallic complex of anthracene shown in Figure 1. The two crystallographically equivalent $(C_5Me_5)_2Sm$ units are located on either side of the nearly planar $C_{14}H_{10}$ moiety as shown in Figure 2. The average Sm–C(C_5Me_5) distance (2.72(2) Å) and the Cn–Sm–Cn angle (134.8°, Cn = centroid of the C_5Me_5 ring) (Table 4) are normal for nine-coordinate Sm(III) complexes.[23] It should be noted that

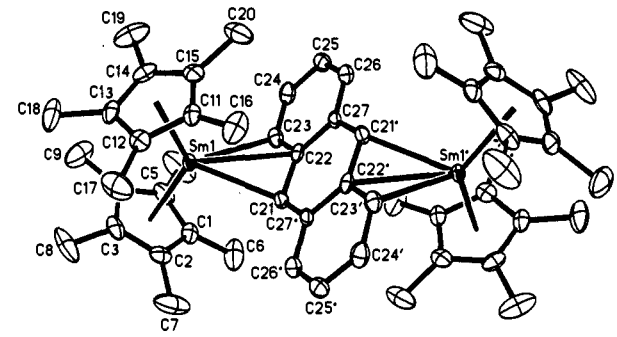

Figure 1. Thermal ellipsoid plot diagram of $[(\eta^5\text{-}C_5Me_5)_2Sm]_2[\mu\text{-}\eta^3\text{:}\eta^3\text{-}(C_{14}H_{10})]$ (**2**) with thermal ellipsoids drawn at the 50% probability level.

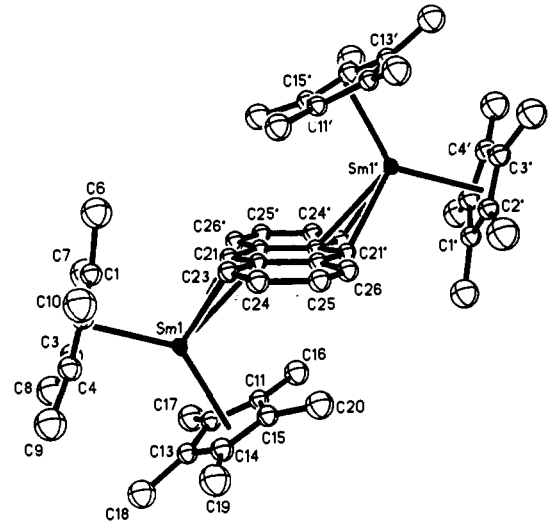

Figure 2. Side view of $[(\eta^5\text{-}C_5Me_5)_2Sm]_2[\mu\text{-}\eta^3\text{:}\eta^3\text{-}(C_{14}H_{10})]$ (**2**).

(19) Evans, W. J.; Ulibarri, T. A.; Ziller, J. W. *J. Am. Chem. Soc.* **1988**, *110*, 6877–6879.
(20) de Boer, E. *Adv. Organomet. Chem.* **1964**, *2*, 115–155.
(21) Evans, W. J.; Gonzales, S. L.; Ziller, J. W. *J. Am. Chem. Soc.* **1991**, *113*, 7423–7424.
(22) Evans, W. J.; Ulibarri, T. A.; Ziller, J. W. *J. Am. Chem. Soc.* **1987**, *109*, 4292–4297.
(23) Evans, W. J.; Foster, S. E. *J. Organomet. Chem.* **1992**, *433*, 79–94.

Table 4. Selected Bond Distances (Å) and Angles (deg) for $[(\eta^5\text{-}C_5Me_5)_2Sm]_2[\mu\text{-}\eta^3\text{:}\eta^3\text{-}(C_{14}H_{10})]$ (**2**), $(\eta^5\text{-}C_5Me_5)_2Sm]_2[\mu\text{-}\eta^3\text{:}\eta^3\text{-}(C_{16}H_{10})]$ (**3**), and $[(\eta^5\text{-}C_5Me_5)_2[\mu\text{-}\eta^3\text{:}\eta^3\text{-}(C_{18}H_{12})]$ (**4**)

complex[a]		2		3			4
Sm–C(ring)		2.721(22)		2.726(25)			2.719(24)
Sm–Cn		2.427		2.436	2.429		2.413
		2.462		2.461	2.449		2.465
Sm–C(polycyclic)	Sm–C(21)	2.595(4)	Sm(2)–C(46)	2.660(4)		Sm–C(21)	2.708(12)
			Sm(1)–C(41)	2.664(4)			
	Sm–C(22)	2.791(4)	Sm(1)–C(42)	2.791(4)		Sm–C(22)	2.828(10)
			Sm(2)–C(45)	2.806(4)			
	Sm–C(23)	2.840(4)	Sm(1)–C(43)	2.723(4)		Sm–C(23)	2.688(11)
			Sm(2)–C(44)	2.736(4)			
Cn–Sm–Cn		134.8		134.4	134.7		134.3
C(poly)–Sm–C(poly)	C(21)–Sm–C(23)	55.3(1)	C(41)–Sm(1)–C(43)	55.2(1)		C(21)–Sm–C(23)	55.2(4)
			C(44)–Sm(2)–C(46)	55.3(1)			
C–C–C(poly)	C(21)–C(22)–C(23)	122.2(4)	C(44)–C(45)–C(46)	122.8(3)		C(21)–C(22)–C(23)	123.8(10)
			C(41)–C(42)–C(43)	123.1(3)			

[a] Cn = centroid of C_5Me_5 ring.

Table 5. Planarity and Perpendicular Displacement of Samarium from the Polycyclic Ligand

complex	2	3	4	7	8
deviation from planarity (Å)	±0.02	±0.01	±0.02	±0.02	±0.26
distance of Sm from plane (Å)	2.037	2.094	2.063	1.616	1.161
		2.143			
angle between Sm and polycyclic plane (deg)	122	117	121	136	141
		120			

if a Sm(II) center were present, a distinctly different Sm–C average distance would be expected.[23] Hence, the structural data are consistent with the ^{13}C NMR shifts which are indicative of a Sm(III) complex.

The $C_{14}H_{10}$ unit is planar to within ±0.02 Å and each samarium lies 2.037 Å from this plane (Table 5). The closest approach of the $(C_5Me_5)_2Sm$ unit to the anthracene ring involves C(21) (C(9) in free anthracene). The 2.595(4) Å Sm(1)–C(21) distance in **2** is slightly longer than the Sm–C single bonds in $(C_5Me_5)_2SmMe(THF)$[13a] (2.484(14) Å) and $(C_5Me_5)_2SmPh(THF)$[24] (2.511(8) Å), but it is shorter than the Sm–C(alkene) distances in the styrene complex, $[(C_5Me_5)_2Sm]_2(CH_2CHPh)$[8] (2.674(15) and 2.732(15) Å). This Sm(1)–C(21) distance is in the range of the shortest Sm–C(allyl) distances found in the allyl complexes, $(C_5Me_5)_2Sm(\eta^3\text{-}CH_2CHCHR)$[25] (2.551(17)–2.643(3) Å, R = H, Me, Ph). The 2.791(4) Å Sm–C(22) and 2.840(4) Å Sm–C(23) distances are also within the overall range of Sm–C(allyl) distances found in these allyl complexes (2.551(17)–2.922(3) Å). The closest samarium–hydrogen contacts in **2** are the 2.570 and 2.654 Å distances involving the hydrogen atoms on C(23) and C(21), respectively. In comparison, Sm–H bond distances of 2.05(11) and 2.11(9) Å have been observed in $(C_5Me_5)_2Sm(\mu\text{-}H)(\mu\text{-}CH_2C_5Me_4)Sm(C_5Me_5)$[26] and the close Sm···H contacts in $[(C_5Me_5)_2Sm]_2(PhNNPh)$ are 2.29–2.34 Å.[27]

Lanthanide ligand contact distances in compounds that contain cyclopentadienyl rings as well as other π-bound ligands can best be evaluated by comparing the average Ln–C(C_5R_5) distance, which clearly represents a significant interaction, to other Ln–C(unsaturated hydrocarbon) distances in the structure.[8] Ln–C(hydrocarbon) interactions at distances 0.1–0.2 Å greater than the Ln–C(C_5Me_5) average in the same complex generally show little perturbation of the hydrocarbon structure.[8,28] Since the Sm(1)–C(21) distance in **2** is 0.13 Å *shorter* than the Sm–C(C_5Me_5) average, this interaction appears to be the most significant. The Sm(1)–C(22) and Sm(1)–C(23) distances are 0.07 and 0.12 Å longer, respectively, than the average Sm–C(C_5Me_5) distance and are expected to be correspondingly less important. However, as described above, these distances are comparable to those observed in samarium allyl complexes. The Sm–C(anthracene) distances in **2** can also be compared with the 2.88(2) and 2.90(4) Å average Sm–C(ring) distances found in the η^6-arene complexes, $Sm(\eta^6\text{-}C_6Me_6)(AlCl_4)_3$[5] (2.89(5) Å) and $Sm(\eta^6\text{-}m\text{-}Me_2C_6H_4)(AlCl_4)_3$,[6] respectively.

Comparison of the structural parameters in **2** can also be made with the main group structures of $[(Me_2NCH_2CH_2NMe_2)Li]_2C_{14}H_{10}$ (**9**),[29] $[(THF)_3Mg(\mu\text{-}H)AlEt_2](C_{14}H_{10})$ (**10**),[30] $(THF)_3Mg[9,10\text{-}(Me_3Si)_2C_{14}H_8]$ (**11**),[31] $(THF)_3Mg(1,4\text{-}Me_2C_{14}H_8)$ (**12**),[32] $\{(THF)_2Mg[9,10\text{-}(Me_3Si)_2C_{14}H_8]\}\{(Me_2NCH_2CH_2NMe_2)Mg[9,10\text{-}(Me_3Si)_2C_{14}H_8]\}$ (**13**),[33] $(THF)_3Mg(C_{14}H_{10})$ (**14**),[34] and the recently reported $(C_5H_5)(THF)_2Lu(C_{14}H_{10})$ (**15**),[35] and $[(C_5H_5)_2Lu(C_{14}H_{10})][Na(diglyme)_2]$ (**16**).[36] All of these complexes differ significantly from **2** in that the tricyclic unit is no longer planar. In **9**, one of the lithium atoms is roughly centered over the center ring and the other is centered over an adjacent ring on the opposite side of the anthracene dianion. In **10–16**, the metal is located closest to the positions equivalent to C(21) and C(21′) in Figure 1 (these are C(9) and C(10) in anthracene). These carbon atoms exhibit the characteristics of sp^3 hybridization and the outer rings deviate significantly from planarity. The extent of nonplanarity increases from the lithium to the magnesium and lutetium complexes with the angles between the outer two C_6 rings as follows: 14.7° (**9**), 31.3° (**10**), 45° (**11**), 41° (**12**), 42.9° and 41.2° (**13**), 26.6° and 30.6° (**14**), 29.9 and 38.7° (**15**), and 40.1° (**16**). Hence, **2** represents a new geometry for an organometallic anthracene dianion complex.

(24) Evans, W. J.; Bloom, I.; Hunter, W. E.; Atwood, J. L. *Organometallics* **1985**, *4*, 112–119.
(25) Evans, W. J.; Ulibarri, T. A.; Ziller, J. W. *J. Am. Chem. Soc.* **1990**, *112*, 2314–2324.
(26) Evans, W. J.; Ulibarri, T. A.; Ziller, J. W. *Organometallics* **1991**, *10*, 134–142.
(27) Evans, W. J.; Drummond, D. K.; Chamberlain, L. R.; Doedens, R. J.; Bott, S. G.; Zhang, H.; Atwood, J. L. *J. Am. Chem. Soc.* **1988**, *110*, 4983–4994.
(28) (a) Burns, C. J.; Andersen, R. A. *J. Am. Chem. Soc.* **1987**, *109*, 915–917. (b) Burns, C. J.; Andersen, R. A. *J. Am. Chem. Soc.* **1987**, *109*, 941–942.
(29) Rhine, W. E.; Davis, J.; Stucky, G. *J. Am. Chem. Soc.* **1975**, *97*, 2079–2085.
(30) Lehmkuhl, H.; Mehler, K.; Benn, R.; Rufińska, A.; Schroth, G.; Krüger, C. *Chem. Ber.* **1984**, *117*, 389–403.
(31) Lehmkuhl, H.; Shakoor, A.; Mehler, K.; Krüger, C.; Angermund, K.; Tsay, Y.-H. *Chem. Ber.* **1985**, *118*, 4239–4247.
(32) Bogdanović, B.; Janke, N.; Krüger, C.; Mynott, R.; Schlichte, K.; Westeppe, U. *Angew. Chem. Int. Ed. Engl.* **1985**, *24*, 960–961.
(33) Alonso, T.; Harvey, S.; Junk, P. C.; Raston, C. L.; Skelton, B. W.; White A. H. *Organometallics* **1987**, *6*, 2110–2116.
(34) Engelhardt, L. M.; Harvey, S.; Raston, C. L.; White, A. H. *J. Organomet. Chem.* **1988**, *341*, 39–51.
(35) Roitershtein, D. M.; Ellern, A. M.; Antipin, M. Y.; Rybakova, L. F.; Struchkov, Y. T.; Petrov, E. S. *Mendeleev Commun.* **1992**, 118–120.
(36) Roitershtein, D. M.; Rybakova, L. F.; Petrov, E. S.; Ellern, A. M.; Antipin, M. Y.; Struchkov, Y. T. *J. Organomet. Chem.* **1993**, *460*, 39–45.

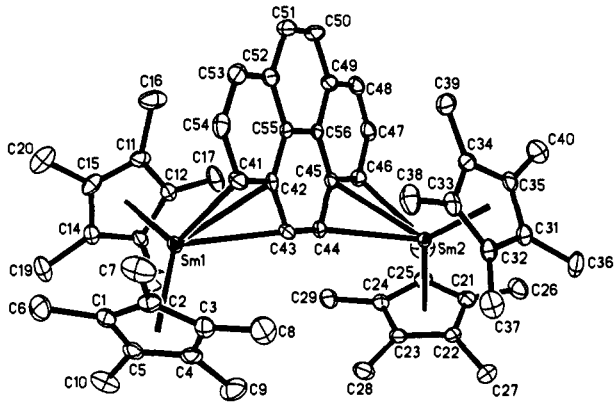

Figure 3. Thermal ellipsoid plot diagram of $[(\eta^5\text{-}C_5Me_5)_2Sm]_2[\mu\text{-}\eta^3\text{:}\eta^3\text{-}(C_{16}H_{10})]$ (**3**) with thermal ellipsoids drawn at the 50% probability level.

The shortest Sm–C distances in **2** can be compared with the metal carbon distances in **10–16** after the differences in metallic radii are considered. In **12** and **14**, which are the most pertinent magnesium complexes since the carbon atoms attached to the metal are unsubstituted, magnesium carbon distances range from 2.25(1) to 2.32 Å. Since the ionic radius of five coordinate Mg(II) is 0.42 Å smaller than the ionic radius of eight coordinate Sm(III),[37] an equivalent Sm–C(21) distance in **2** would be 2.67–2.79 Å. Given the 2.595(4) Å Sm–C distance in **2**, this suggests a more substantial metal ring interaction than in the magnesium compounds. It was similarly concluded in the study of **15** and **16** that the metal ligand interaction was more substantial with the lanthanide, lutetium, than with magnesium.[36] In **15**, the Lu–C distances are 2.44(1) and 2.45(1) Å and the ionic radius of seven coordinate Lu(III) is 0.16 Å smaller than the ionic radius of eight coordinate Sm(III).[37] In **16**, the Lu–C distances are 2.473(6) and 2.482(6) Å and the ionic radius of eight-coordinate Lu(III) is 0.102 Å smaller than the ionic radius of eight-coordinate Sm(III).[37] These distances suggest that the lutetium-carbon atom interactions in **15** and **16** are comparable to the Sm–C(21) interaction in **2**, despite the fact that **2** is more allylic in character and **15** and **16** are essentially σ-bonded dialkyl species. The bond distance changes in the anthracene dianion in **2** and **9–16** are remarkably similar considering the different bonding modes involved. In all of these cases the shorter bonds in free anthracene[38] lengthen and the longer bonds shorten. A molecular orbital rationale for this pattern has been presented.[29]

The Pyrene Reaction. Formation of $[(\eta^5\text{-}C_5Me_5)_2Sm]_2[\mu\text{-}\eta^3\text{:}\eta^3\text{-}(C_{16}H_{10})]$ (3). Addition of 0.5 equiv of pyrene to **1** in toluene also caused an immediate color change, in this case, to bright green. Removal of solvent gave a dark green complex which analyzed as an analog of **2**, namely $[(\eta^5\text{-}C_5Me_5)_2Sm]_2[\mu\text{-}\eta^3\text{:}\eta^3\text{-}(C_{16}H_{10})]$ (**3**), eq 2. Like **2**, addition of THF to **3** regenerated

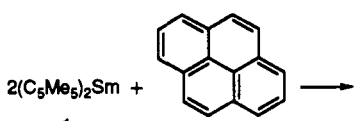

$$[(C_5Me_5)_2Sm]_2[\mu\text{-}\eta^3\text{:}\eta^3\text{-}(C_{16}H_{10})] \quad (2)$$
3

the polycyclic aromatic hydrocarbon and formed $(C_5Me_5)_2Sm(THF)_2$. The identity of **3** was confirmed by an X-ray diffraction study, Figure 3. The ^1H NMR spectrum of **3** differed from that of **2** in that it contained a single resonance in the C_5Me_5 region.

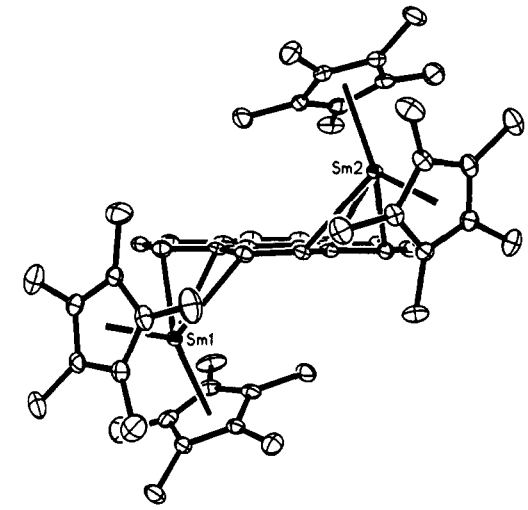

Figure 4. Side view of $[(\eta^5\text{-}C_5Me_5)_2Sm]_2[\mu\text{-}\eta^3\text{:}\eta^3\text{-}(C_{16}H_{10})]$ (**3**).

Although the structures of **2** and **3** are similar in that two $(C_5Me_5)_2Sm$ units are located on either side of the polycyclic ring as shown in Figure 4, **3** is unusual in that the two samarium units are positioned at the same end of the molecule. As in **2**, the pyrene unit in **3** is planar (to within ±0.01 Å) and the samarium atoms are 2.094 and 2.143 Å from this plane. **3** is also similar to **2** in that three Sm–C(polycyclic ligand) interactions are in the same range of distances found in the allyl complexes, $(C_5Me_5)_2Sm(CH_2CHCHR)$.[25] The range of these distances is smaller than the range in **2**: the shortest distances in **3**, 2.660 (4) and 2.664 (4) Å, are longer than the shortest distance in **2** (2.595(4) Å), and the longest distances, the 2.791(4) Sm(1)–C(42) and 2.806(4) Å Sm(2)–C(45) lengths, are shorter than the longest Sm–C(23) distance in **2** (2.840(4) Å, Table 4). Furthermore, these long distances in **3** involve the carbon atom in the middle of the pseudo-allyl component of the polycyclic hydrocarbon, whereas the long distance in **2** involves an end carbon. In **3**, both of the end carbon atoms in the pseudo-allyl unit have Sm–C distances less than or equal to the average Sm–C(C_5Me_5) distance, 2.73(2) Å.

Few pyrene complexes are available in the literature for comparison. $[(Os(NH_3)_5)_2(\mu\text{-}\eta^2\text{:}\eta^2\text{-pyrene})](OTf)_4$[39] is known, but it is unlike **3** in that the two metal centers are symmetrically disposed about the polycyclic ligand and attach by interacting only with individual C–C bonds. The osmium centers are ca. 2 Å out of the plane of the pyrene ligand which is planar to within ±0.08 Å. The Os–C(pyrene) distances (2.169(15) and 2.175(14) Å) are ca. 0.49 Å shorter than the analogous Sm–C(pyrene) distances in **3**, a difference which is close to the 0.45 Å difference in their ionic radii.[37]

The 2,3-Benzanthracene Reaction. Formation of $[(\eta^5\text{-}C_5Me_5)_2Sm]_2[\mu\text{-}\eta^3\text{:}\eta^3\text{-}(C_{18}H_{12})]$ (4). The reaction of **1** with 2,3-benzanthracene produces an immediate color change from dark green to kelly green and **4** can be isolated in quantitative yield like **2** and **3**. **4** was characterized by elemental analysis and fully identified by X-ray crystallography as $[(\eta^5\text{-}C_5Me_5)_2Sm]_2[\mu\text{-}\eta^3\text{:}\eta^3\text{-}(C_{18}H_{12})]$, eq 3, Figure 5. This complex, like **2**, had a ^1H NMR spectrum containing two C_5Me_5 resonances.

As in **2**, the two crystallographically equivalent $(C_5Me_5)_2Sm$ units in **4** are located on either side of the nearly planar $C_{18}H_{12}$ moiety. The $C_{18}H_{12}$ unit is planar to within ±0.02 Å and each samarium lies 2.063 Å from this plane. The 2.719(24) Å average Sm–C(C_5Me_5) distance in **4** is also similar to that in **2** and **3**. However, in **4** the closest approach of the $(C_5Me_5)_2Sm$ unit to the 2,3-benzanthracene ring involves the two carbon atoms, C(23) and C(21), at distances of 2.688(10) and 2.708(12) Å, and the

(37) Shannon, R. D. *Acta Crystallogr.* **1976**, *A32*, 751–767.
(38) Brock, C. P.; Dunitz, J. D. *Acta Crystallogr.* **1990**, *B46*, 795–806.
(39) Hasegawa, T.; Sekine, M.; Schaefer, W. P.; Taube, H. *Inorg. Chem.* **1991**, *30*, 449–452.

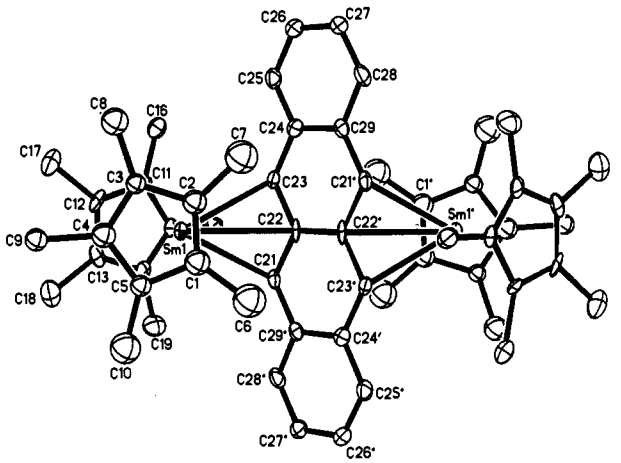

Figure 5. Thermal ellipsoid plot diagram of $[(\eta^5\text{-}C_5Me_5)_2Sm]_2[\mu\text{-}\eta^3\text{:}\eta^3\text{-}(C_{18}H_{12})]$ (4) with thermal ellipsoids drawn at the 50% probability level.

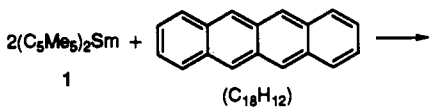

$$2(C_5Me_5)_2Sm + (C_{18}H_{12}) \longrightarrow [(C_5Me_5)_2Sm]_2[\mu\text{-}\eta^3\text{:}\eta^3\text{-}(C_{18}H_{12})] \quad (3)$$

1 4

Sm–C distance for the carbon atom in between, C(22), is 2.828-(10) Å. Hence, **4** has a structure more similar to that of **3** than **2** (Table 4). A further difference between **4** and **2** is that the two $(C_5Me_5)_2Sm$ moieties are directly across from each other in **4** rather than being offset as in **2**. The arrangement is such that each $(C_5Me_5)_2Sm$ unit has its closest contacts with carbon atoms formally equivalent to C(21) and C(21′) in **2**.

The 9-Methylanthracene and Acenaphthylene Reactions. Formation of $[(C_5Me_5)_2Sm]_2(C_{15}H_{12})$ (5) and $[(C_5Me_5)_2Sm]_2(C_{12}H_8)$ (6). Both 9-methylanthracene and acenaphthylene react with **1** via immediate color changes to form new complexes in high yield, eqs 4 and 5. In both cases, elemental analyses were consistent

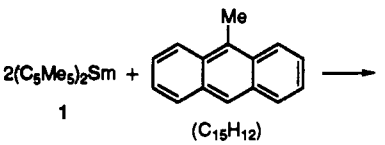

$$2(C_5Me_5)_2Sm + (C_{15}H_{12}) \longrightarrow [(C_5Me_5)_2Sm]_2(C_{15}H_{12}) \quad (4)$$

1 5

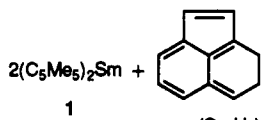

$$2(C_5Me_5)_2Sm + (C_{12}H_8) \longrightarrow [(C_5Me_5)_2Sm]_2(C_{12}H_8) \quad (5)$$

1 6

with the formation of 2:1 Sm:polycyclic hydrocarbon complexes as was found for **2**. In contrast to **2**, which is green in solution and purple-black as a microcrystalline solid, **5** is intensely dark red in solution and in the solid state. The acenaphthylene complex, **6**, is dark blue. **5** also differs from **2** in that it has a single C_5Me_5 resonance in its ^1H NMR spectrum (like **3**) and it is more soluble in arenes than **2**. The ^1H NMR spectrum of **6** is like that of **2** and **4** in that two C_5Me_5 ^1H NMR resonances are present. Unfortunately, the NMR data are not structurally definitive and without single crystals little can be said about the structure of **5** and **6**.

The Coronene and Azulene Reactions. Addition of 0.5 equiv of coronene, $C_{24}H_{12}$, to **1** caused no apparent reaction. However, the low solubility of coronene may inhibit this reaction. When

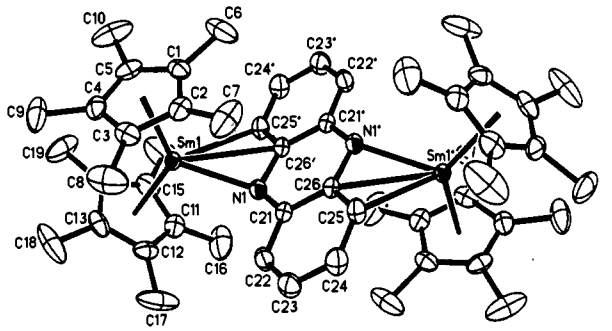

Figure 6. Thermal ellipsoid plot diagram of $[(\eta^5\text{-}C_5Me_5)_2Sm]_2[\mu\text{-}\eta^3\text{:}\eta^3\text{-}(C_{12}H_8N_2)]$ (7) with thermal ellipsoids drawn at the 50% probability level.

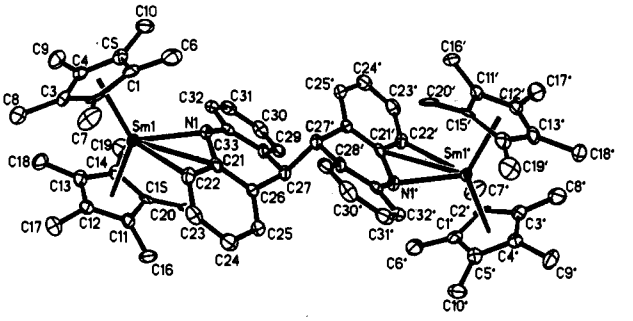

Figure 7. Thermal ellipsoid plot diagram of $[(\eta^5\text{-}C_5Me_5)_2Sm]_2[\mu\text{-}\eta^3\text{:}\eta^3\text{-}(C_{13}H_9N)_2]$ (8) with thermal ellipsoids drawn at the 50% probability level.

0.5 equiv of azulene, $C_{10}H_8$, is added to a green benzene solution of **1**, an immediate color change occurs to give a reddish-brown solution. In contrast to eqs 1–5, ^1H NMR analysis indicates that there are two products present in the reaction mixture: the known complex $(C_5Me_5)_3Sm$[21] and a new product which displayed a single C_5Me_5 resonance. In contrast to the products discussed above, addition of THF to this mixture did not regenerate azulene and form $(C_5Me_5)_2Sm(THF)_2$. Unfortunately, the two products were not readily separated and it was not possible to fully establish the identity of the second product. The formation of $(C_5Me_5)_3$-Sm has a parallel in the reaction of 1,3,5,7-cyclooctatetraene with **1**, eq 6,[21] and by analogy it is likely that the other product of the azulene reaction is $(C_5Me_5)Sm(C_{10}H_8)$.

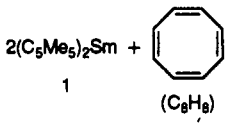

$$2(C_5Me_5)_2Sm + (C_8H_8) \longrightarrow (C_5Me_5)Sm(C_8H_8) + (C_5Me_5)_3Sm \quad (6)$$

1

The Phenazine Reaction. Formation of $[(\eta^5\text{-}C_5Me_5)_2Sm]_2[\mu\text{-}\eta^3\text{:}\eta^3\text{-}(C_{12}H_8N_2)]$ (7). Phenazine, which has a reduction potential of –0.364,[40] reacts with **1** in a reaction analogous to eq 1 and a reddish-brown 2:1 Sm:substrate complex, $[(\eta^5\text{-}C_5Me_5)_2Sm]_2[\mu\text{-}\eta^3\text{:}\eta^3\text{-}(C_{12}H_8N_2)]$ (7), eq 7, analogous to **2** was isolated in

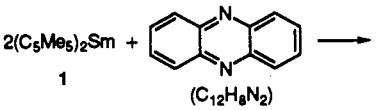

$$2(C_5Me_5)_2Sm + (C_{12}H_8N_2) \longrightarrow [(C_5Me_5)_2Sm]_2[\mu\text{-}\eta^3\text{:}\eta^3\text{-}(C_{12}H_8N_2)] \quad (7)$$

1 7

quantitative yield. The X-ray diffraction study revealed a structure similar to the anthracene complex, **2** (Figure 6): **7** is a bimetallic complex, the metal centers are offset to the side of

(40) Nechaeva, O. N.; Pushkareva, Z. V. *Zh. Obshch. Khim.* **1958**, *28*, 2693–2701. *Chem. Abst.* **1959**, 9229d.

Table 6. Selected Bond Distances (Å) and Angles (deg) for $[(\eta^5\text{-}C_5Me_5)Sm]_2[\mu\text{-}\eta^3\text{:}\eta^3\text{-}(C_{12}H_8N_2)]$ (**7**) and $[(\eta^5\text{-}C_5Me_5)_2Sm]_2[\mu\text{-}\eta^3\text{:}\eta^3\text{-}(C_{13}H_9N)_2]$ (**8**)

complex		**7**		**8**
Sm–C(ring)		2.708(12)		2.713(15)
Sm–Cn		2.436		2.416
		2.421		2.443
Sm–N		2.360(2)		2.380(5)
Sm–C(heterocycle)	Sm–C(25′)	2.866(3)	Sm–C(22)	2.944(5)
	Sm–C(26′)	2.877(2)	Sm–C(21)	2.970(5)
Cn–Sm–Cn		136.4		136.3
N–Sm–C(heterocycle)	N–Sm–C(25′)	53.8(1)	N–Sm–C(22)	52.4(1)
N–C–C(heterocycle)	N–C(26′)–C(25′)	118.9(2)	N–C(21)–C(22)	118.6(4)

[a] Cn = centroid of C_5Me_5 ring.

the π-system, the phenazine unit retains its planarity to within ±0.02 Å, and the interaction with the ring system appears to be allylic. In **7**, however, the shortest metal ligand distance is now between the samarium centers and the nitrogen atoms at the 9 and 10 positions of the phenazine ring. Just as the Sm–C(21) distance in **2** is slightly longer than a typical $(C_5Me_5)_2Sm$–C bond, the 2.360(2) Å Sm(1)–N(1) distance in **7** is slightly longer than the 2.301(3) Å Sm–N distance in $(C_5Me_5)_2Sm[N(SiMe_3)_2]$[41] (Table 6). The closest Sm–H contact for **7** is 2.471 Å (Sm(1)–H(25A)). **7** differs from **2** in that the perpendicular displacement of the samarium atom from the hydrocarbon plane is smaller (1.62 vs. 2.04 Å) and the angle between the plane formed by samarium, N(1), and C(25′) and the plane of the polycyclic is larger for **7**, 136°, than for **2** (122°). **7** also differs from **2** in that its ^{1}H NMR spectrum exhibits only one resonance in the C_5Me_5 region.

The structure of **7** can be compared to that of the magnesium complex, $[Mg_2Br_2(C_{12}H_8N_2)(THF)_6][MgBr_2(THF)_4]$ (**17**), which contains a phenazine dianion.[42] As in the anthracene dianion complexes described above, the magnesium complex is significantly different from the samarium system. In **17**, the phenazine dianion is essentially σ bonded to the magnesium and functions as an amido ligand. The 2.052(7) Å Mg–N distance would be equivalent to a 2.472 Å Sm–N distance after differences in radial size are considered,[37] which again shows a more substantial interaction with samarium than with magnesium.

The Acridine Reaction. Formation of $[(\eta^5\text{-}C_5Me_5)_2Sm]_2[\mu\text{-}\eta^3\text{:}\eta^3\text{-}(C_{13}H_9N)_2]$ (8). When 0.5 equiv of acridine, which has a reduction potential of –0.618,[40] is added to **1** in toluene, an instantaneous color change to orange is observed. Despite the reaction stoichiometry, a coupled product with a 1:1 Sm:substrate ratio was isolated: $[(\eta^5\text{-}C_5Me_5)_2Sm]_2[\mu\text{-}\eta^3\text{:}\eta^3\text{-}(C_{13}H_9N)_2]$ (**8**) (Figure 7). **8** is formed in quantitative yield according to eq 8. Unlike **7**, two C_5Me_5 resonances are observed in the ^{1}H NMR spectrum of **8**.

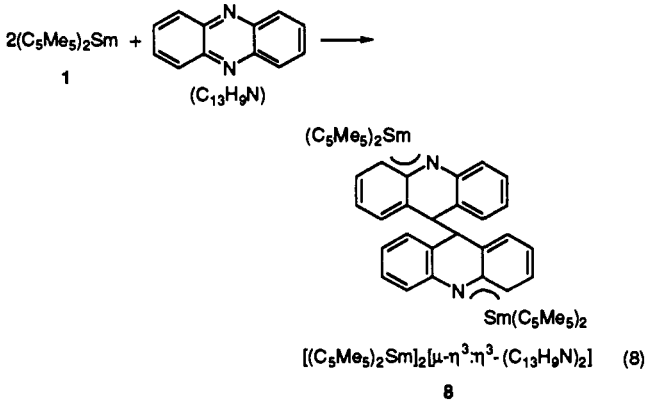

$[(C_5Me_5)_2Sm]_2[\mu\text{-}\eta^3\text{:}\eta^3\text{-}(C_{13}H_9N)_2]$ (8)

8

The 2.380(5) Å Sm–N distance of **8**, like that of **7**, is also slightly longer than the 2.301(3) Å Sm–N single bond distance found in $(C_5Me_5)_2Sm[N(SiMe_3)_2]$,[41] but it is substantially shorter than the average Sm–C(C_5Me_5) distance in **8** (2.713(15) Å) (Table 6). The Sm–C(21) and Sm–C(22) distances are at the long end of the range of Sm–C(allyl) distances previously observed. The polycyclic ligand in **8** exhibits a larger deviation from planarity (±0.26 Å) than any of the previously discussed complexes for which structural data have been obtained. The perpendicular displacement of the Sm metals in **8** from the plane containing the polycyclic ligand, 1.161 Å, is smaller than that in complexes **2–4** and **7** and the angle formed by the plane containing the samarium, N(1), and C(22) and the acridine plane is the largest (141°).

Discussion

Reactivity. As shown in Table 3, $(C_5Me_5)_2Sm$ (**1**) reacts with a variety of polycyclic aromatic hydrocarbons. From the reduction potentials of the reactive polycyclic systems and the fact that **1** can reduce stilbene,[8] it appears that **1** can form isolable reduced products with polycyclic aromatics which have reduction potentials equal to or more positive than –2.22 V. The fact that double reduction of anthracene and pyrene occurs suggests that the substrates with reduction potentials as negative as –2.44 V may react with **1**. These data are consistent with previous estimates[12,43] of the reduction potential of $(C_5Me_5)_2Sm(THF)_x$ (x = 0–2) complexes.[2,10,44] It should be noted, however, that the appropriate reduction potentials alone will not ensure formation of a new product, since no isolable product was obtained with the poorly soluble coronene.

Reduction of polycyclic aromatic hydrocarbons by **1** appears to be rapid. In each of the reactions which generated **2–8**, *i.e.*, eqs 1–8, immediate color changes occurred upon mixing and the products could be isolated in nearly quantitative yield after short reaction times. Although a color change is a good indicator of reactivity, the intense dark green color of **1** can sometimes mask the formation of a new product, particularly if the new product has a green color. This was the case for complexes **2**, **3**, and **4**.

Each reaction was accompanied by a change in the ^{1}H NMR spectrum in which the broad resonance for the C_5Me_5 protons of divalent $(C_5Me_5)_2Sm$ shifted and narrowed into the range typical for trivalent $(C_5Me_5)_2Sm$ moieties. The ^{13}C NMR spectra of these complexes all clearly indicated the presence of trivalent $(C_5Me_5)_2Sm$ moieties by their characteristic shifts.[22] The ^{1}H NMR spectra of **2**, **4**, **6**, and **8** contained the two C_5Me_5 resonances of equal intensity expected from the solid-state structure. However, in the ^{1}H NMR spectra of **3**, **5**, and **7**, only a single C_5Me_5 resonance was found. This situation is similar to that of the allyl complexes $(C_5Me_5)_2Sm(\eta^3\text{-}H_2CCHCH_2)$ and $(C_5Me_5)_2Sm(\eta^3\text{-}MeHCCHCH_2)$.[25] The former complex displays the two

(41) Evans, W. J.; Keyer. R. A.; Ziller, J. W. *Organometallics* **1993**, *12*, 2618–1633.
(42) Junk, P. C.; Raston, C. L.; Skelton, B. W.; White, A. H. *J. Chem. Soc., Chem. Commun.* **1987**, 1162–1164.
(43) Morss, L. R. *Chem. Rev.* **1976**, *76*, 827–841.
(44) (a) Evans, W. J.; Bloom, I.; Hunter, W. E.; Atwood, J. L. *J. Am. Chem. Soc.* **1981**, *103*, 6507–6508. (b) Evans, W. J.; Grate, J. W.; Choi, H. W.; Bloom, I.; Hunter, W. E.; Atwood, J. L. *J. Am. Chem. Soc.* **1985**, *107*, 941–946.

expected C_5Me_5 resonances, but only a single line is observed for the latter species. Neither spectrum changed as the temperature was varied.

The intense colors of **2–6** are not typical for ordinary Sm(III) complexes. Most trivalent $(C_5Me_5)_2SmZ$ complexes in which Z is a halide or pseudohalide are yellow or orange. However, in recent years an increasing number of intensely colored complexes containing trivalent $(C_5Me_5)_2Sm$ moieties have been identified. In general these involve ligands with unusual bonding characteristics and an expectation of some significant charge transfer between the metal and the ligand. Examples include $[(C_5Me_5)_2Sm]_2(\eta^2\text{-}N_2Ph_2)$[27] (dark blue), $[(C_5Me_5)_2Sm]_2(C_2Ph_2)$[45] (black), and $(C_5Me_5)_2Sm(Me_3CN{=}CHCH{=}NCMe_3)$ (dark brown).[46]

For most of the substrates examined in this study, double reduction of the polycyclic aromatic hydrocarbon occurs to give a bimetallic complex of general formula $[(C_5Me_5)_2Sm]_2$(substrate). Formation of such 2:1 complexes is a hallmark of the reactivity of $(C_5Me_5)_2Sm$ and its solvated analogs $(C_5Me_5)_2Sm(THF)$[10] and $(C_5Me_5)_2Sm(THF)_2$ and occurs regardless of the initial reagent stoichiometry.[3] Apparently, the radical formed by the initial reduction of the hydrocarbon by 1 equiv of $(C_5Me_5)_2Sm$ rapidly reacts with a second equivalent of $(C_5Me_5)_2Sm$ to form the observed product.

The $(C_5Me_5)_2Sm(THF)_x$ complexes also have two less common modes of reactivity with unsaturated hydrocarbon substrates and each of these was observed in this study. With some substrates, the initial hydrocarbon reduction is followed by coupling of the hydrocarbon radicals via C–C bond formation. This is observed in the formation of the 1:1 product $(C_5Me_5)_2Sm[\mu\text{-}\eta^4\text{-}(PhHC{=}NNCHPh\text{-})_2]$[47] from benzaldehyde azine and $[(C_5Me_5)_2Sm]_2[\mu\text{-}\eta^4\text{-}(CH{=}NNCH{=}CH\text{-})_2]$[47] from pyridazine. A similar reaction occurs with acridine, eq 8.

The other less common mode of $(C_5Me_5)_2Sm$/hydrocarbon reactivity is one involving ligand redistribution to form $(C_5Me_5)_3Sm$[21] and a monocyclopentadienyl complex, $(C_5Me_5)Sm$(substrate dianion). The only example of this reaction previously in the literature is the instantaneous reaction of **1** with 1,3,5,7-cyclooctatetraene.[48] It is likely that azulene reacts similarly. It is interesting to note that each of the polycyclic substrates in this study has the potential to couple at the radical stage and each dianion could form a monocyclopentadienyl complex via ligand redistribution, yet for each substrate a single quantitative reaction path dominates to give just one type of product.

Structure. The reactions described here have generated a new family of structural types for reduced polycyclic aromatic hydrocarbons. The most unusual feature of the structures of the complexes reported here is the planarity of the reduced hydrocarbon unit. Planar structures have not been reported previously for organometallic complexes of polycyclic aromatic hydrocarbon anions. The several magnesium and lutetium anthracene structures which have been reported,[29–36] all of which are nonplanar, show most dramatically the unusual nature of the $(C_5Me_5)_2Sm$ system. The nonplanarity of anthracene dianion structures has previously been correlated with covalency.[36] However, given the significant differences between the $(C_5Me_5)_2Sm$ complex **2** and the $(C_5H_5)_2Lu$ and $(C_5H_5)(THF)_2Lu$ moieties in **15** and **16**, it appears that the degree of planarity can be controlled by varying the ligand set on the metal. This then is another example of how the proper combination of lanthanide metal and ligands set can vary the chemistry observed.[49]

These reactions reveal that in interacting with polycyclic aromatic hydrocarbons, the $(C_5Me_5)_2Sm$ unit prefers neither the η^6 interactions, which are common for transition metals and also for lithium,[29] nor the dialkyl interactions, which are found for magnesium[30–34] and lutetium.[35–36] Instead, in complexes **2–4**, the $(C_5Me_5)_2Sm$ unit adopts an orientation with the hydrocarbon which is very similar to that found in the allyl complexes $(C_5Me_5)_2Sm(RCHCHCH_2)$.[25] As described above, the bond distances are similar between these sets of complexes and even the dihedral angles between the hydrocarbon and the plane defined by the samarium and the two outer atoms in the allyl interaction are very similar. These angles are 109.3–119.1° in the allyl compounds $((C_5Me_5)_2Sm(CH_2CHCHR)$, R = H, Me, Ph),[25] 118–122° for complexes **2–4**, and 136–141° for complexes **7** and **8**. It is likely that the allylic bonding contributes to maintaining the planarity of the reduced hydrocarbon unit.

Conclusion

$(C_5Me_5)_2Sm$ reduces polycyclic aromatic hydrocarbons with reduction potentials more positive than −2.22 V to form bimetallic complexes of general formula $[(C_5Me_5)_2Sm]_2$(substrate dianion). The $(C_5Me_5)_2Sm$ unit confers sufficient solubility and crystallinity to these species that they can be fully characterized by X-ray crystallography. The structural studies show that the dianions are planar and that the two $(C_5Me_5)_2Sm$ units are attached via an allylic interaction, two features which are unusual for organometallic complexes of reduced polycyclic aromatic hydrocarbons.

Acknowledgment. We thank the National Science Foundation for support for this research and the Graduate Professional Opportunities Program for a dissertation fellowship (to S.L.G.).

Supplementary Material Available: Thermal ellipsoid plots and tables of crystal data, positional parameters, bond distances and angles, and thermal parameters (68 pages). This material is contained in many libraries on microfiche, immediately follows this article in the microfilm version of the journal, and can be ordered from the ACS; see any current masthead page for ordering information.

(45) Evans, W. J.; Bloom, I.; Hunter, W. E.; Atwood, J. L. *J. Am. Chem. Soc.* **1983**, *105*, 1401–1403.

(46) Recknagel, A.; Noltemeyer, M.; Edelmann, F. T. *J. Organomet. Chem.* **1991**, *410*, 53–61.

(47) Evans, W. J.; Drummond, D. K. *J. Am. Chem. Soc.* **1989**, *111*, 3329–3335.

(48) $(C_5Me_5)_2Sm(THF)_2$ reacts with cyclooctatraene to form $(C_5Me_5)_2Sm(C_8H_8)(THF)$ but in this case no $(C_5Me_5)_3Sm$ was observed.[45]

(49) Evans, W. J.; Engerer, S. C.; Piliero, P. A.; Wayda, A. L. In *Fundamental Research in Homogeneous Catalysis*; Tsutsui, M., Ed.; Plenum Press: New York, 1979, Vol. 3, pp 941–952.